2024

Evaluating the Performance of 5G NR in Indoor Environments: An Experimental Study

Bikash Chandra Singh
Old Dominion University, bsingh@odu.edu

Rafael Diaz
Old Dominion University, rdiaz@odu.edu

Sachin Shetty
Old Dominion University, sshetty@odu.edu

Original Publication Citation
Singh, B. C., Diaz, R., & Shetty, S. (2024). Evaluating the performance of 5G NR in indoor environments: An experimental study. *Procedia Computer Science*, *241*, 16-23. https://doi.org/10.1016/j.procs.2024.08.005

Available online at www.sciencedirect.com

ScienceDirect

Procedia Computer Science 241 (2024) 16–23

Procedia Computer Science

www.elsevier.com/locate/procedia

The 19th International Conference on Future Networks and Communications (FNC)
August 5-7, 2024, Marshall University, Huntington, WV, USA

Evaluating the Performance of 5G NR in Indoor Environments: An Experimental Study

Bikash Chandra Singh[a,*], Rafael Diaz[a], Sachin Shetty[b]

[a] *School of Cybersecurity, Old Dominion University, Norfolk, VA 23529, USA*
[b] *Virginia Modeling, Analysis, and Simulation Center (VMASC), Old Dominion University, Suffolk, VA 23435, USA*

Abstract

The 5G wireless standard has emerged as a trans-formative technology with the potential to revolutionize various industries by providing enhanced connectivity and communication capabilities. This advanced standard offers a diverse range of applications, including Ultra-Reliable Low-Latency Communication (URLLC), Enhanced Mobile Broadband (eMBB), and Massive Machine Type Communication (mMTC). In this scientific research paper, we present a comprehensive analysis of the performance and capabilities of a deployed indoor 5G network in a controlled laboratory environment. The experimental setup comprises an Amarisoft Callbox, serving as the 5G core, along with a Remote Radio Head (RRH) and user equipment (UEs). Our primary objective is to assess the network's performance by evaluating the downlink, uplink, and joint downlink/uplink transmissions for TCP and UDP protocols between the gNodeB and user equipment (UE). To achieve this, we carefully examine key performance metrics such as latency, power consumption, CPU utilization, and signal quality. Through various configurations that involve MIMO 2 technology and a 30 kHz sub-carrier spacing, we investigate the impact of different NR Bandwidth settings. By establishing TCP and UDP connections for both uplink and downlink scenarios, we meticulously measure and scrutinize the system's performance, thereby providing valuable insights into its efficiency and suitability for diverse application requirements.

Keywords: Indoor 5G; Latency; CPU utilization; Power consumption; Signal quality

1. Introduction

The proliferation of wireless communication technologies has led to an ever-increasing demand for high-speed and reliable connectivity, particularly in indoor environments. In response to this demand, the development and deployment of 5G New Radio (NR) systems have gained significant attention. 5G NR offers enhanced performance and capabilities compared to its predecessors, making it a promising solution for meeting the connectivity needs of indoor environments. Indoor 5G NR systems aim to provide seamless connectivity, ultra-low latency, and high data rates to support a wide range of applications. These applications include Ultra-Reliable Low-Latency Communication (URLLC), which caters to critical applications such as industrial automation; Enhanced Mobile Broadband

* Corresponding author. Tel.: +0-000-000-0000 ; fax: +0-000-000-0000.
E-mail address: bsingh@odu.edu

10.1016/j.procs.2024.08.005

(eMBB), which delivers high-speed internet access and multimedia services; and Massive Machine Type Communication (mMTC), which enables the Internet of Things (IoT) and the interconnection of numerous devices [1, 2].

However, indoor environments pose challenges with intricate radio propagation conditions, hindering 5G signals from permeating obstacles like walls and furniture. This obstacle penetration issue often results in diminished signal quality and degraded performance. Ensuring optimal performance in indoor 5G NR systems demands a comprehensive performance evaluation and optimization analysis. Numerous studies have extensively explored the integration of 5G with other communication systems. For example, in [12], we conducted brief experiments on 5G NR for Indoor environments. In [4], authors examined the coexistence of 5G NR and 4G LTE in the C-Band. Seamless coverage through 5G and 4G uplink coexistence in the C-band was discussed in [3]. Furthermore, [5] provided an in-depth analysis of predictive latency in 5G networks using real-world network data. A. Sahbafard et al. [6] presented an experimental 5G standalone deployment based on the OpenAirInterface, evaluating coverage parameters for single and multiple user scenarios. Conversely, [7] focused on a private 5G IoMusT deployment, analyzing its performance in supporting Networked Music Performance (NMP). In [8], authors deployed a 5G network configured to meet V2X latency requirements, using cooperative lane change as a case study. These studies collectively contribute to the understanding and enhancement of 5G system performance in diverse scenarios. In [9], a thorough analysis delves into the coexistence performance of 5G New Radio (5G NR), 4G Long Term Evolution Advanced Pro (LTE-A Pro), and Narrowband Internet of Things (NB-IoT) in the 700 MHz Band, exploring both co-channel and adjacent channel scenarios. Meanwhile, [10] proposes a design approach for 5G-NR radio planning, covering both FR1 and FR2, with a focus on outdoor and indoor areas. The paper outlines the calculation of the required number of base stations for installation. Moreover, [11] provides an overview of electromagnetic field (EMF) exposure assessment concerns arising from 5G-related measurement campaigns in Austria, Italy, and Malaysia. The paper further presents results from short and long-term experimental analyses conducted within the 5G-frequency ranges, namely FR1 and FR2.

In this paper, we comprehensively analyze the performance of indoor 5G NR systems, focusing on key metrics such as latency, data rate, power consumption, CPU utilization, and signal quality across diverse scenarios and configurations. Our study considers influential factors like antenna placement, base station distance, user density, and channel conditions. Utilizing commercial off-the-shelf (COTS) equipment, we construct and deploy an indoor 5G NR testbed for our analysis. Through extensive experiments, we scrutinize the impact of various parameters, providing insights into the capabilities and limitations of indoor 5G NR systems. Our findings enhance understanding of their performance characteristics and offer valuable deployment optimization guidelines for real-world indoor environments. In summary, our contributions in this paper are:

- The paper investigates and measures the latency between gNodeB and UE by fine-tuning resource allocation and ACK/Nack parameters. More particularly, it adjusts the number of time slots between PDSCH/DCI and uplink data transmission for improving the latency performance.
- In this paper, we compute CPU utilization and cell capacity for DL and UL transmissions, considering TCP and UDP connections between gNodeB and UE. This analysis provides valuable insights into the network's efficiency and capacity under different transmission scenarios.
- The paper estimates the power consumption of Remote Radio Head (RRH) and gNode separately. This assessment helps in understanding the power requirements in indoor 5G NR systems.
- The experimental results demonstrate the signal quality between gNodeB and UEs at varying distances that paving the way for future advancements in 5G network optimization.

The remainder of this paper is organized as follows: Section 2 provides the network setup of indoor 5G NR systems. Section 3 presents the results and analysis of our performance evaluation. Finally, Section 4 concludes the paper with a summary of the findings and directions for future research.

2. Network Setup

In this paper, we unveil the architecture of our indoor 5G system, illustrated in Figure 1. The experimental setup involves multiple User Equipment (UEs) communicating with a single gNodeB. UEs transmit UDP and TCP data packets to a Simbox application server, employing Software Defined Radio (SDR) technology for communication. Each SDR card supports MIMO2x2, featuring 2 RX, 2 TX, and 1 GPS SMA connectors. Our setup includes the Amarisoft NR (SA) Simbox, a Callbox acting as a 3GPP compliant eNB/gNB and EPC/5GC, and a client PC with the Amarisoft Web User Interface (WUI). The Callbox, configured with default settings in the gnb-sa.cfg file, facilitates functional and performance testing of 5G NSA and SA devices. The Simbox, configured using the ue-nr-sa.cfg file, enables UE simulation with shared spectrum. Wireless links connect the Simbox and Callbox, while the client PC interfaces with the Simbox via an Ethernet cable. The Amarisoft WUI allows monitoring and visualization of virtual UEs emulated from the Simbox in our 5G testbed environment.

In order to extend the coverage of our indoor 5G network and enable connectivity for real User Equipment (UEs), we have integrated a 5G Remote Unit (RU) into our system. The RU is connected to the Amarisoft Callbox via CPRI ports, utilizing an optical link. To establish seamless communication between the UEs and the gNodeB, we have deployed an omnidirectional antenna, which facilitates the connection of UEs to the gNodeB through the RU. To ensure the optimal performance and functionality of our network, we have carefully configured the necessary parameters in the gnb-sa.cfg and ue-nr-sa.cfg configuration files, as outlined in Table 1. Specifically, our network configuration encompasses the utilization of 2x2 Multiple-Input Multiple-Output (MIMO) technology and cell bandwidths of 20 MHz and 50 MHz. It is worth noting that the reference to cell bandwidth corresponds to the aggregated cell bandwidth, which is determined by multiplying the number of Downlink (DL) MIMO layers by the NR (New Radio) bandwidth. For instance, a configuration of 2x2 MIMO and 20 MHz of cell bandwidth results in an aggregated cell bandwidth of 40 MHz, while a configuration of 2x2 MIMO and 50 MHz cell bandwidth yields an aggregated cell bandwidth of 100 MHz.

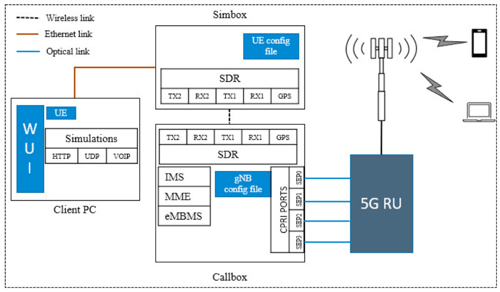

Fig. 1: Indoor 5G NR Systems

Table 1: Network parameters

Network parameters	Values
# DL Antenna	2
# UL Antenna	1
NR Bandwidth	20 MHz, 50 MHz
Tx_gain	90 dB
Rx_gain	60 dB
Subcarrier spacing	30 kHz
Synchronization Signal Block (SSB) Period	20 ms

Table 2: System's CPU Specification

Parameters	Values
CPU architecture	X86_64
CPU core	16
Thread(s) per core	2
Core(s) per socket	8

3. Results and Discussion

3.1. End-to-End latency measurement

In our experimental exploration, we intricately fine-tuned key parameters of the 5G network within our testbed to achieve optimal end-to-end latency. A pivotal adjustment involved shortening the Scheduling Request Period (sr_period) to minimize waiting time for UEs to obtain UL Grants, thereby promoting more efficient communication with the gNB. Additionally, we optimized the configuration of the Physical Random-Access Channel (PRACH) by exclusively allocating RACH Occasions (RO) on UL symbols, enhancing PRACH utilization efficiency and overall system performance. The K_min value, specifically k1 and k2 parameters, was carefully set to expedite UE responses, improving transmission efficiency between the gNB and UEs. To evaluate end-to-end latency, UEs were categorized into idle and busy phases. During the busy phase, HTTP packets were forwarded from UEs to the network, and subsequent pinging measured latency. In the idle phase, where UEs were not actively transmitting data, latency measurements were conducted via pinging. The experiments were conducted on two setups: i) Amarisoft 5G systems and ii) integrated 5G systems with Amarisoft and AW2S Remote Radio Head (RRH).

The experimental outcomes, illustrated in Figure 2 and Figure 3, show that when UE(s) were idle, and the Scheduling Request Period (sr_period) was set to 2 and 1 with k_min at 4, the latency ranged from 6.97ms (minimum) to 10.42ms (maximum). Real UE(s) exhibited slightly higher latency, around 10ms (minimum) and 14.4ms (maximum), compared to Simbox-simulated UE(s) in Amarisoft 5G systems. Our findings also revealed that larger k_min and sr_period values in the 5G Standalone (SA) network correlated with increased latency. Specifically, a k_min value of 8 and sr_period at 40 resulted in higher latency in the 5G NR SA network. Additionally, the integrated 5G systems with Amarisoft and AW2S RRH exhibited slightly higher latency than the standalone Amarisoft setup. However, the

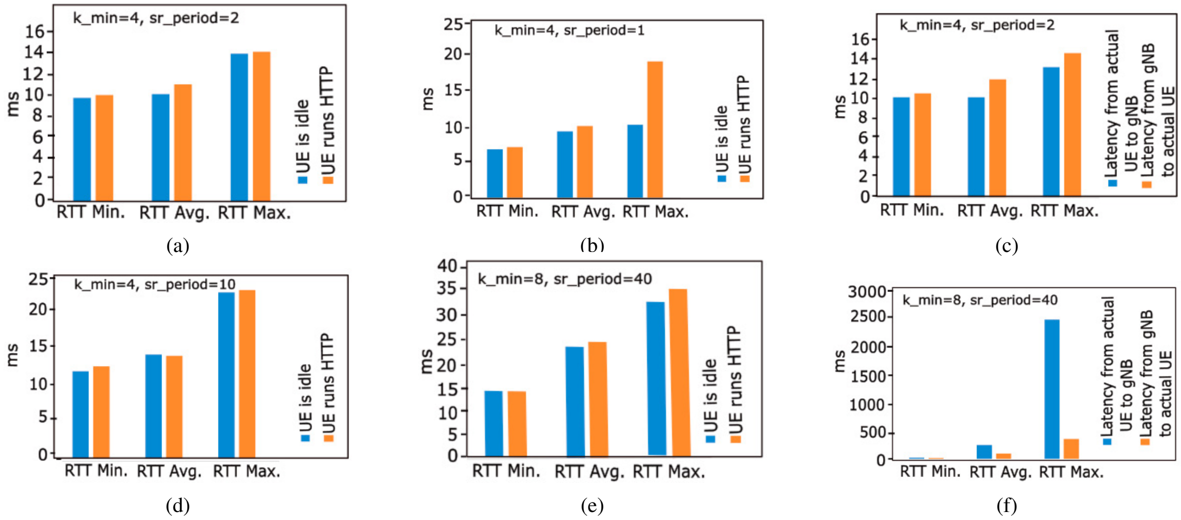

Fig. 2: Latency obtained with Amarisoft 5G NR for various k_min and sr_period values when UE's idle and busy

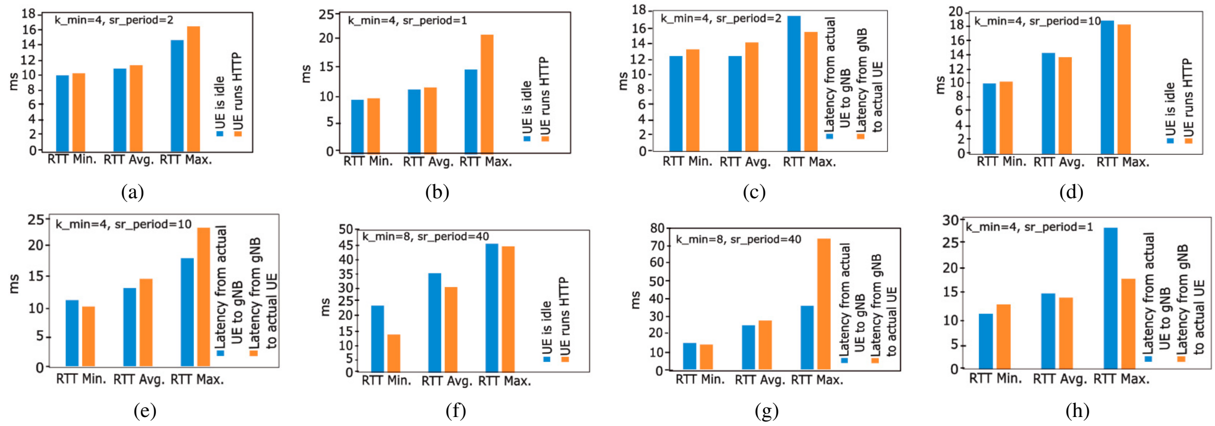

Fig. 3: Latency obtained with integrated 5G NR of AW2S RRH and Amarisoft 5G for various k_min and sr_period values when UE's idle and busy

integrated 5G systems demonstrated superior network coverage, making it a favorable option for specific deployment scenarios despite a modest impact on latency.

3.2. Cell Capacity and CPU Utilization

In order to measure the cell capacity and CPU utilization, we conducted experiments for i) Downlink (DL) and ii) Uplink (UL) transmissions. These experiments were performed on the integrated 5G NR of AW2S RRH and Amarisoft equipped with specific CPU specifications, which are listed in Table 2.

DL test. We performed a straightforward evaluation with MIMO CAT 4 at 150 Mbps in UDP. For this, the iPerf command used in server mode on the UE side was: "iperf -s -u -i 1", while iPerf in client mode on the core network PC, the command was: "iperf -c <UE IP address> -u -b 150M -i 1 -t 20". In addition, for TCP connections, iPerf was initiated in server mode at UE side, and on the core network PC, we employed the following commands, respectively: iperf -s -i 1, iperf -c <UE IP address> -i 1 -t 20.

UL test. For UL transmission, we conducted a simple uplink test in MIMO CAT 4 at 50 Mbps using UDP on our core network PC with this command: iperf -s -u -i 1 and ran iPerf in client mode at the UE side with this command: iperf -c <PDN Gateway IP address> -u -b 50M -i 1 -t 100. Additionally, we performed another experiment with a TCP connection using iPerf command. More particularly, at the core network PC side, we ran the following command: iperf -s -i 1, and at the UE side: iperf -c <PDN GATEWAY IP address> -i 1 -t 100.

DL and UL run concurrently. This experiment assesses gNodeB CPU utilization through concurrent uplink and downlink tests. Using the iperf tool for both UDP and TCP connections, we initiated UDP data transmission from the core network PC with the command “iperf -c < UE IP address > -d -u -b 150M -I 1 -t 20”. Simultaneously, at the UE side, we ran “iperf -s -u -i 1” to receive UDP packets. For TCP connection, we utilized the command “iperf -c <UE IP address> -d -i 1 -t 20” on the core network PC, with the UE side serving as the server, receiving TCP packets through “iperf -s -I 1”.

Table 3: Power Consumption by RRH

Interval (sec)	Aggregated Cell Bandwidth (MHz)	Trans. Link	Packet type	Antenna(s)	Power type	Power in dBm (Approx.))
20	20x2=40	DL	UDP	ANT0	Output power	26.6
					Input power	−86.8 ± 2.4
				ANT0/TX	Maximum power	30.0
					Measured Power	26.5
				ANT0/RX	Measured power	−90.9 ± 2.5
			TCP	ANT0	Output power	26.7
					Input power	−87.7 ± 1.4
				ANT0/TX	Maximum power	30.0
					Measured Power	26.5
				ANT0/RX	Measured power	−90.9 ± 2.5
20	20x2=40	UL	UDP	ANT0	Output power	12.6
					Input power	−72.8 ± 2.1
				ANT0/TX	Maximum power	30.0
					Measured Power	12.4
				ANT0/RX	Measured power	−94.8 ± 0.1
			TCP	ANT0	Output power	10.0
					Input power	−89.8 ± 1.0
				ANT0/TX	Maximum power	30.0
					Measured Power	14.5
				ANT0/RX	Measured power	−73.2 ± 1.6
20	20x2=40	UL and DL	UDP	ANT0	Output power	26.7
					Input power	−70.0 ± 3.0
				ANT0/TX	Maximum power	30.0
					Measured Power	26.6
				ANT0/RX	Measured power	−73 ± 3
			TCP	ANT0	Output power	26.7
					Input power	−73 ± 2
				ANT0/TX	Maximum power	30.0
					Measured Power	26.6
				ANT0/RX	Measured power	−70 ± 2
20	50x2=100	DL	UDP	ANT0	Output power	0
					Input power	−72.0 ± 8.0
				ANT0/TX	Maximum power	30.0
					Measured Power	26.2
				ANT0/RX	Measured power	−77 ± 1.2
			TCP	ANT0	Output power	0
					Input power	−80 ± 10.2
				ANT0/TX	Maximum power	30.0
					Measured Power	29.2
				ANT0/RX	Measured power	−76.9 ± 2
20	50x2=100	UL	UDP	ANT0	Output power	0
					Input power	−60 ± 10
				ANT0/TX	Maximum power	30.0
					Measured Power	9.1
				ANT0/RX	Measured power	−56 ± 3.9
			TCP	ANT0	Output power	0
					Input power	−57 ± 2
				ANT0/TX	Maximum power	30.0
					Measured Power	10.6 ± 2
				ANT0/RX	Measured power	−62.1 ± 4
20	50x2=100	UL and DL	UDP	ANT0	Output power	26.6
					Input power	−68 ± 1.5
				ANT0/TX	Maximum power	30.0
					Measured Power	26.4
				ANT0/RX	Measured power	−71 ± 2.3
			TCP	ANT0	Output power	26.8
					Input power	−67 ± 3
				ANT0/TX	Maximum power	30.0
					Measured Power	26.6 ± 2
				ANT0/RX	Measured power	−70.0 ± 1

Table 4: Power Consumption by gNodeB

Interval (sec)	Aggregated Cell Bandwidth (MHz)	Trans. Link	Packet type	TX MAX	TX SAT	RX RMS	RX MAX
20	20x2=40	DL	UDP	−3.7 to −3.0	0	−62.8 to −62.2	−40.4 to −36.9
			TCP	−3.9 to −2.6	0	−59.1 to −57.1	−33.0 to −27.2
		UL	UDP	−6.4 to −5.1	0	−42.5 to −40.8	−28.0 to −25.0
			TCP	−7.3 to −3.7	0	−41.1 to −39.8	−27.5 to −25.3
		UL and DL	UDP	−2.8 to −3.5	0	−33.8 to −44.0	−30.7 to −33.9
			TCP	−2.8 to −3.7	0	−41.4 to −44.7	−25.9 to −30.1
	50x2=100	DL	UDP	−2.6 to −1.4	0	−50.2 to −45.9	−28.3 to −18.8
			TCP	−2.3 to −1.5	0	−47.2 to −40.5	−22.7 to −14.9
		UL	UDP	−10.3 to −9.9	0	−33.2 to −25.3	−9.7 to −3.1
			TCP	−10.5 to −9.9	0	−35.1 to −32.0	−16.5 to −12.7
		UL and DL	UDP	−3.1 to −3.5	0	−39.3 to −40.8	−24.7 to −26.0
			TCP	−2.2 to −3.1	0	−37.3 to −41.0	−20.8 to −26.4

Table 5: Received signal power at gNodeB

Rx gain (dBm)	RX frequency (MHz)	RX power (dBm)
40	3389	−82
	3489	−60.5
	3589	−81
60	3389	−85
	3489	−67.3
	3589	−83.3.3

Table 6: CPU utilization and data rate

Interval (sec)	Aggregated Cell Bandwidth (MHz)	Transmission Link	Packet type	Data Rate (Mbps)	Proc/CPU (dBm)	RX/CPU (dBm)	TX/ CPU(dBm)
20	20x2=40	DL	UDP	74 ± 2.4	41.9 ± 3.4(%)	1.7(%)	2.95± 0.15(%)
			TCP	70.3 ± 1.5	42.0 ± 4.7(%)	1.7(%)	3.3 ± 0.1(%)
		UL	UDP	28.6	50 ± 4.2(%)	1.8(%)	3.0 ± 0.2(%)
			TCP	22 ± 10.3	48 ± 1.9(%)	1.8(%)	2.7 ± 0.2(%)
		UL and DL	UDP	60	50 ± 3(%)	1.8(%)	2.7 ± 0.2(%)
			TCP	50	53 ± 3(%)	1.8(%)	2.6 ± 0.2(%)
	50x2=100	DL	UDP	155 ± 2	64 ± 3.4(%)	3.0(%)	4.3 ± 0.2(%)
			TCP	271 ± 10	69 ± 5.4(%)	3.0(%)	4.3 ± 0.2(%)
		UL	UDP	52.3 ± 1.0	71 ± 2.8(%)	3.0(%)	4.5 ± 0.1(%)
			TCP	55.8	79 ± 2.5(%)	3.0(%)	4.5 ± 0.1(%)
		UL and DL	UDP	188	106 ± 2(%)	3.0(%)	4.4 ± 0.1(%)
			TCP	178.8	112 ± 6(%)	3.0(%)	4.3 ± 0.2(%)

Table 6 presents the experimental results using the specified commands for UDP and TCP connections, varying cell bandwidths. Key metrics measured include Proc/CPU, RX/CPU, TX/CPU, and bandwidth. Proc/CPU signifies the total CPU load of the gNodeB process, while RX/CPU and TX/CPU denote the time spent on reading and writing IQ samples from/to the RF driver, respectively. Our findings indicate higher data rates for downlink (DL) operations compared to uplink (UL) operations across all cases, with UL operations requiring greater CPU utilization. Further analysis using s-tui tools examines CPU core utilization for DL and UL transmissions with aggregated cell bandwidths of 40 MHz and of 100MHz. Figure 4 displays detailed results from our 5G testbed, revealing increased CPU utilization with larger cell bandwidths.

3.3. Power Consumption measurement

In this section, we measured the power consumption of the AW2S Remote Radio Head (RRH 4x4 33 dBm) and the gNodeB of Amarisoft callbox. The objective was to assess the power usage of these components under various cell bandwidth configurations.

Power consumption by Remote Radio Head (RRH). To precisely gauge the RRH power consumption, we employed a radio management unit (RMU). Integrating a transceiver board with the Amarisoft callbox facilitated this

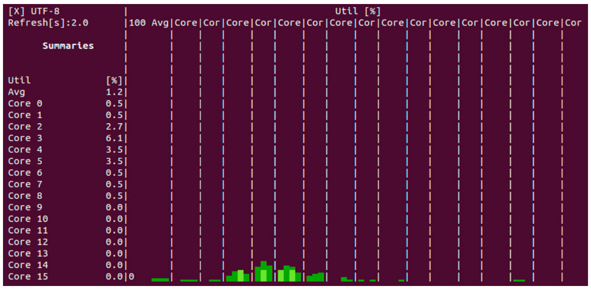

(a) UDP DL with a 40MHz cell bandwidth

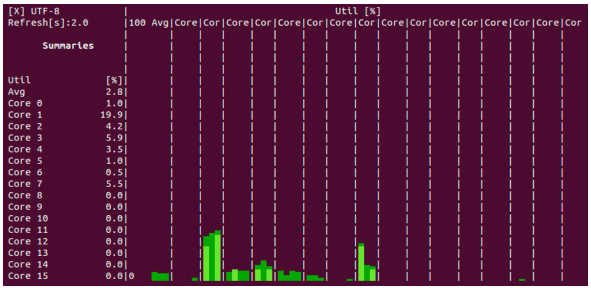

(b) TCP DL with a 40MHz cell bandwidth

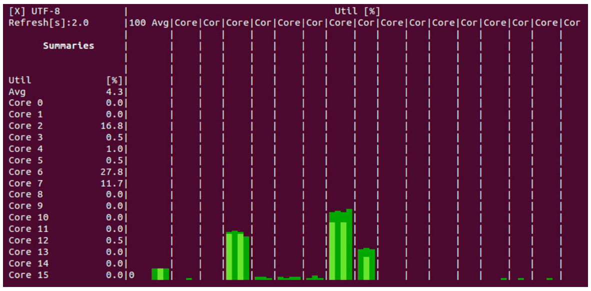

(c) UDP UL with a 40MHz cell bandwidth

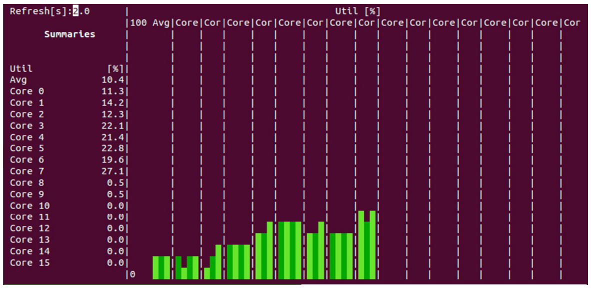

(d) TCP UL with a 40MHz cell bandwidth

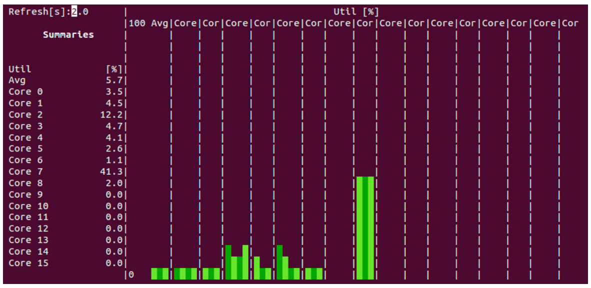

(e) UDP DL & UL with a 40MHz cell bandwidth

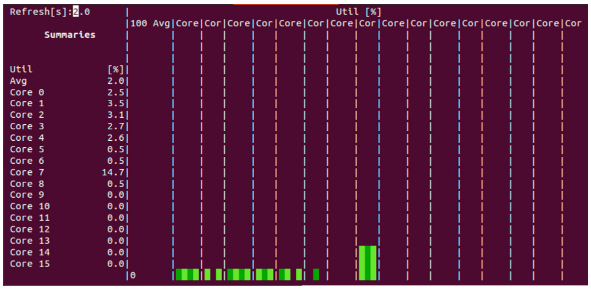

(f) TCP DL & UL with a 40MHz cell bandwidth

Fig. 4: CPU utilization for various transmission types with a 40 MHz cell bandwidth

measurement. The RMU service was initiated using the command “screen -r rmu.” With the RMU service active, we measured the RRH power, revealing a consumption of 87 watts. Separate power assessments were conducted for RRH antennas during downlink (DL) and uplink (UL) transmissions over TCP and UDP connections, each lasting 20 seconds. The results, presented in Table 3, indicated an increase in RRH power consumption with higher frequencies for the gNodeB cell.

Power consumption by gNodeB. We measured the transmitted signal power of gNodeB using “screen -r lte” and “t spl”, respectively. The specific parameters used for power consumption measurement are as follows: i) **TX MAX:** This field specifies the maximum transmitted power in dBm; ii) **TX SAT:** This field represents the number of saturation events that occurred during the measurement period. If the SAT value is not equal to zero (0), it means that the signal transmitted in downlink is saturated; iii) **RX RMS:** This field refers to the received Root Mean Square (RMS) value in dBm; iv) **RX MAX:** This parameter specifies the maximum received power measured in dBm. Table 4 shows the power consumption incurred at gNodeB. From Table 4, it shows that gNodeB requires more power to execute both DL and UL operations when the cell bandwidth is set to 100 MHz compared to 40 MHz.

SDR Spectrum Analyzer at gNodeB. In this section, we analyzed the gNodeB cell spectrum by investigating the receiver functionality of a designated SDR (e.g., SDR0) and confirming the transmission functionality of adjacent SDR cards (e.g., SDR1, SDR2). The analysis involved running gNodeB on SDR0 while employing a spectrum analyzer on another SDR (SDR 1, 2, or 3) to measure the transmitted signal spectrum from the TX port of SDR0. Results for received signal power at different frequencies and RX gains are presented in Table 5 and Figure 5. The experiment involved varying the center frequency of SDR cards within the range of 3389 MHz to 3589 MHz, with RX gains set at

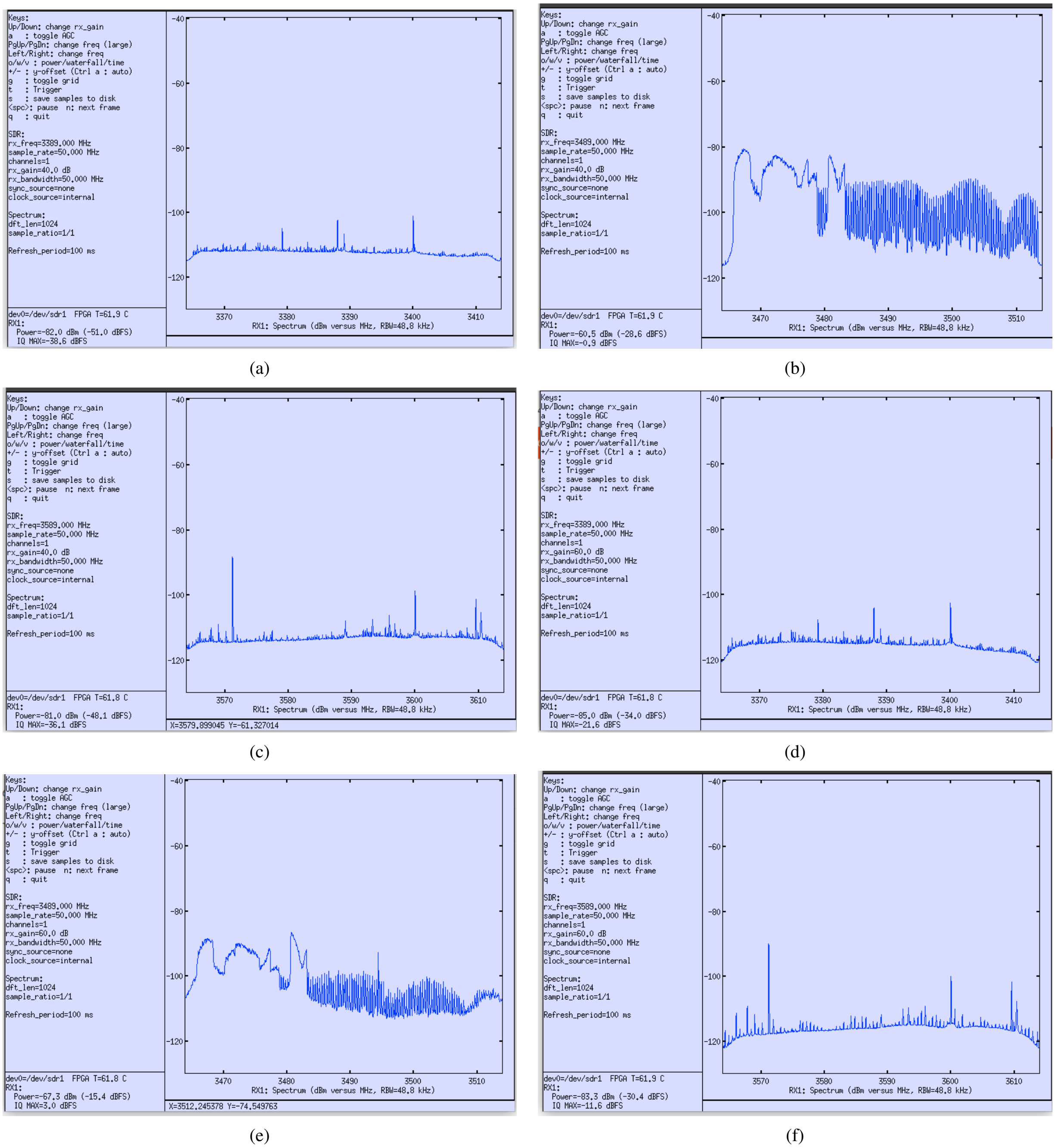

Fig. 5: Spectrum analysis for gNodeB's receiver functionality

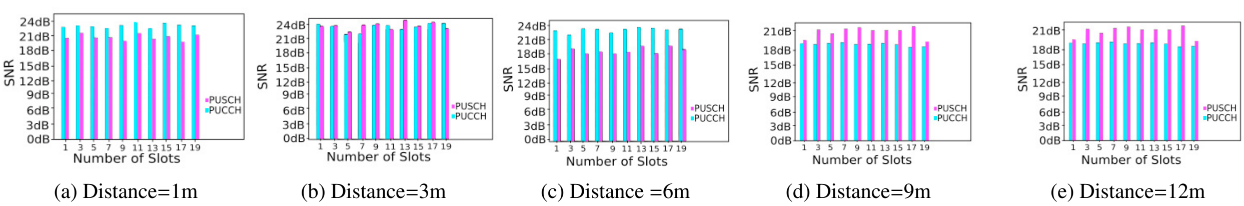

Fig. 6: Signal quality between gNodeB and UE with varying distances

40 dBm and 60 dBm. The findings suggest that 3489 MHz may serve as a more suitable center frequency, exhibiting improved signal reception and requiring less power for transmission.

3.4. Signal Quality Assessment between gNodeB and UEs

This research article delved into the pivotal role of 5G physical channels in enabling seamless communication between User Equipment (UEs) and 5G gNodeBs (base stations). Specifically, we focused on the key uplink channels, namely the Physical Uplink Shared Channel (PUSCH) and the Physical Uplink Control Channel (PUCCH). With 5G NR supporting concurrent transmission on PUSCH and PUCCH, we explored their performance under varying gNodeB-UE distances through experimental measurements. The investigation not only examined the PUSCH's capacity to convey user data and optional Uplink Control Information (UCI) but also analyzed the PUCCH's effectiveness in carrying vital UCI, encompassing Channel State Information (CSI) reports, Hybrid Automatic Repeat Request (HARQ) feedback, and Scheduling Requests (SR). Our findings, presented in Figure 6, illustrated that the Signal-to-Noise Ratio (SNR) for both PUSCH and PUCCH exhibits improved performance as UEs approach closer proximity to the gNodeB.

4. Conclusion

This paper conducts a comprehensive analysis of indoor 5G standalone deployment, emphasizing key performance metrics—latency, data rate, CPU utilization, power consumption, and signal quality. Results show a minimum average Round Trip Time (RTT) of approximately 7 ms and 9 ms for simulated and actual User Equipment (UE) scenarios, respectively, when the UE is not concurrently engaged. The study explores the impact of varied aggregated cell bandwidth on UDP and TCP connections in Downlink (DL) and Uplink (UL) transmissions, consistently demonstrating superior data rate performance for UDP. Larger cell bandwidths increase CPU utilization in the gNodeB. Power consumption patterns of the Remote Radio Head (RRH) and gNodeB reveal a direct correlation between higher cell bandwidth consumption and increased power usage. Signal quality between gNodeB and UE(s) is examined concerning their distance, underscoring the importance of optimal network layout in indoor 5G deployments. These insights offer valuable guidance for future 5G network implementations, particularly addressing challenges related to large aggregated cell bandwidth, with a focus on mitigating latency and power consumption issues.

Acknowledgements

This work is supported by Coastal Virginia node of the Commonwealth Cyber Initiative (COVA CCI). This work is also supported by Grant No. 200398-010.

References

[1] L. Chettri, and B. Rabindranath. (2020) ”A comprehensive survey on Internet of Things (IoT) toward 5G wireless systems.” *IEEE Internet of Things Journal* **7(1)**: 16-32.

[2] S. Sukhmani, M. Sadeghi, M. Erol-Kantarci, and A. E. Saddik. (2018) ”Edge caching and computing in 5G for mobile AR/VR and tactile internet.” *IEEE MultiMedia* **26 (1)**: 21-30.

[3] T. Levanen, K. Ranta-Aho, J. Kaikkonen, S. Nielsen, K. Pajukoski, M. Renfors, and M. Valkama. (2018) ”5G new radio and LTE uplink coexistence.” *IEEE Wireless Commun. Netw. Conf.*, pp. 1–6

[4] L. Wan, Z. Guo, and X. Chen. (2019) ”Enabling efficient 5G NR and 4G LTE coexistence.” *IEEE Wireless Commun* **26(1)**: 6–8.

[5] M. Skocaj, F. Conserva, N. S. Grande, A. Orsi, D. Micheli, G. Ghinamo, R. Verdone. (2023) ”Data-driven Predictive Latency for 5G: A Theoretical and Experimental Analysis Using Network Measurements.” *arXiv preprint arXiv*.

[6] A. Sahbafard, R. Schmidt, F. Kaltenberger, A. Springer, and H. P. Bernhard. (2023) ”On the Performance of an Indoor Open-Source 5G Standalone Deployment.” *IEEE Wireless Communications and Networking Conference (WCNC)*, pp. 1-6.

[7] L. Turchet, and P. Casari. (2023) ”Latency and Reliability Analysis of a 5G-Enabled Internet of Musical Things system.” *IEEE Internet of Things Journal*, DOI 10.1109/JIOT.2023.3288818.

[8] B. Coll-Perales et al. (2023) ”End-to-End V2X Latency Modeling and Analysis in 5G Networks.” *IEEE Transactions on Vehicular Technology* **72(4)**: 5094-5109, doi: 10.1109/TVT.2022.3224614.

[9] L. C. Alexandre, A. L. De Souza Filho and A. C. Sodré. (2020) ”Indoor Coexistence Analysis Among 5G New Radio, LTE-A and NB-IoT in the 700 MHz Band.” *in IEEE Access* **8**: 135000-135010, doi: 10.1109/ACCESS.2020.3011267.

[10] S. Chinkhong and P. Kaewplung. (2023) ”A Design Approach for 5G-NR Radio Planning Using Both FR1 and FR2 on Any Selected Outdoor and Indoor Areas.”*2023 International Conference on Electronics, Information, and Communication (ICEIC)*, Singapore, pp. 1-4, doi: 10.1109/ICEIC57457.2023.10049901.

[11] G. Betta et al. (2023) ”Human exposure to 5G systems: experimental analysis and measurement issues in FR1 and FR2 operating bands.” *2023 IEEE International Instrumentation and Measurement Technology Conference (I2MTC)*, Kuala Lumpur, Malaysia, pp. 01-06, doi: 10.1109/I2MTC53148.2023.10176034.

[12] S. Bikash Chandra et al. (2024, January) ”Performance Analysis of Indoor 5G NR Systems.” *2024 IEEE 21st Consumer Communications & Networking Conference (CCNC)*, Las Vegas, NV, USA, pp. 632-633, doi: 10.1109/CCNC51664.2024.10454767.